

pubs.acs.org/NanoLett Letter

Fabrication of Cellulose—Graphite Foam via Ion Cross-linking and Ambient-Drying

Ruiliu Wang,^a Chaoji Chen,^a Zhenqian Pang,^a Xizheng Wang,^a Yubing Zhou, Qi Dong, Miao Guo, Jinlong Gao, Upamanyu Ray, Qinqin Xia, Zhiwei Lin, Shuaiming He, Bob Foster, Teng Li,* and Liangbing Hu*



Cite This: Nano Lett. 2022, 22, 3931-3938



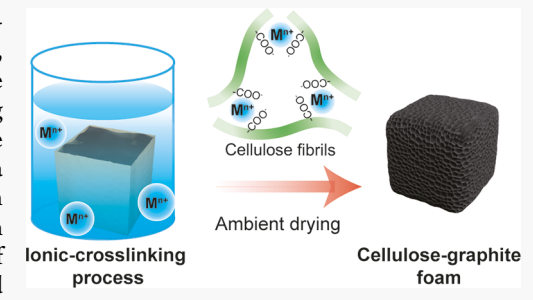
ACCESS

III Metrics & More

Article Recommendations

Supporting Information

ABSTRACT: Conventional plastic foams are usually produced by fossil-fuel-derived polymers, which are difficult to degrade in nature. As an alternative, cellulose is a promising biodegradable polymer that can be used to fabricate greener foams, yet such a process typically relies on methods (e.g., freeze-drying and supercritical-drying) that are hardly scalable and time-consuming. Here, we develop a fast and scalable approach to prepare cellulose—graphite foams via rapidly cross-linking the cellulose fibrils in metal ions-containing solution followed by ambient drying. The prepared foams exhibit low density, high compressive strength, and excellent water stability. Moreover, the cross-linking of the cellulose fibrils can be triggered by various metal ions, indicating good universality. We further use density functional theory to reveal the cross-linking



effect of different ions, which shows good agreement with our experimental observation. Our approach presents a sustainable route toward low-cost, environmentally friendly, and scalable foam production for a range of applications.

KEYWORDS: foam, cellulose, ion cross-linking, ambient drying, water stability

INTRODUCTION

Because of the low density, high specific surface area, low thermal conductivity, and high impact resistance, foam materials are widely used for thermal insulation, 1,2 sound absorption,³ energy storage,⁴ water treatment,⁵ protective packaging,⁶ and so on.⁷ Most commercial foam materials are made of fossil-fuel-based plastics or synthetic polymers, such as polystyrene, polyvinyl chloride, and polyimide, which are not biodegradable in nature and difficult to recycle. To fight the white pollution war, plastic ban has been implemented worldwide and growing efforts have been made for the implementation of sustainable, eco-friendly, and biodegradable polymers to replace the fossil-fuel-based and the synthetic ones.^{9,10} As the most abundant and natural polymer on earth, 11,12 cellulose is a promising candidate to fulfill this goal because of its low cost, low density, high mechanical performance, 13-15 and natural degradability. 16-18 However, large scale manufacturing of cellulose foam is currently limited due to the lack of an efficient and scalable approach, especially for the drying step. ^{19–21} For example, while freeze-drying has been used for the fabrication of cellulose foam containing nanocellular structure in many studies, 22-24 the specialized equipment, long processing time (>48 h), and high energy consumption hinders the scalability of this approach. Although it was shown that cellulose foam with high specific surface area can also be obtained by supercritical drying,²⁵ this method usually involves extreme pressures and substantial use of chemical processing (e.g., dissolving, gelation, and solvent exchange), impairing its practicality for large-scale production. As such, it is critical to develop a facile, efficient, and scalable process for fabrication cellulose foam as a green replacement of the conventional ones.

To meet this need, we develop a fast and scalable approach to prepare cellulose—graphite foams via rapidly cross-linking the cellulose fibrils in metal ions-containing solution followed by ambient drying, where the graphite serves as building blocks of the foam structure. Using this strategy, the foam can be molded into stable shapes with uniform porous structure, exhibiting microcellular structure (average pore size: about 200 μ m), low density (0.036 g·cm⁻³), and excellent water stability. The cross-linking of the cellulose fibrils is promoted by a range of metal ions such as K⁺, Ca²⁺, Zn²⁺, Cu²⁺, Al³⁺, and Fe³⁺, indicating good universality of our method. Density functional theory reveals that the cross-linking effect of different ions follows the order of Ca²⁺ > Fe³⁺ > Al³⁺ > Cu²⁺ > Zn²⁺ > K⁺ > Na⁺, which agrees well with the experimental results. Our

Received: January 17, 2022 Revised: April 5, 2022 Published: May 3, 2022





Nano Letters pubs.acs.org/NanoLett Letter

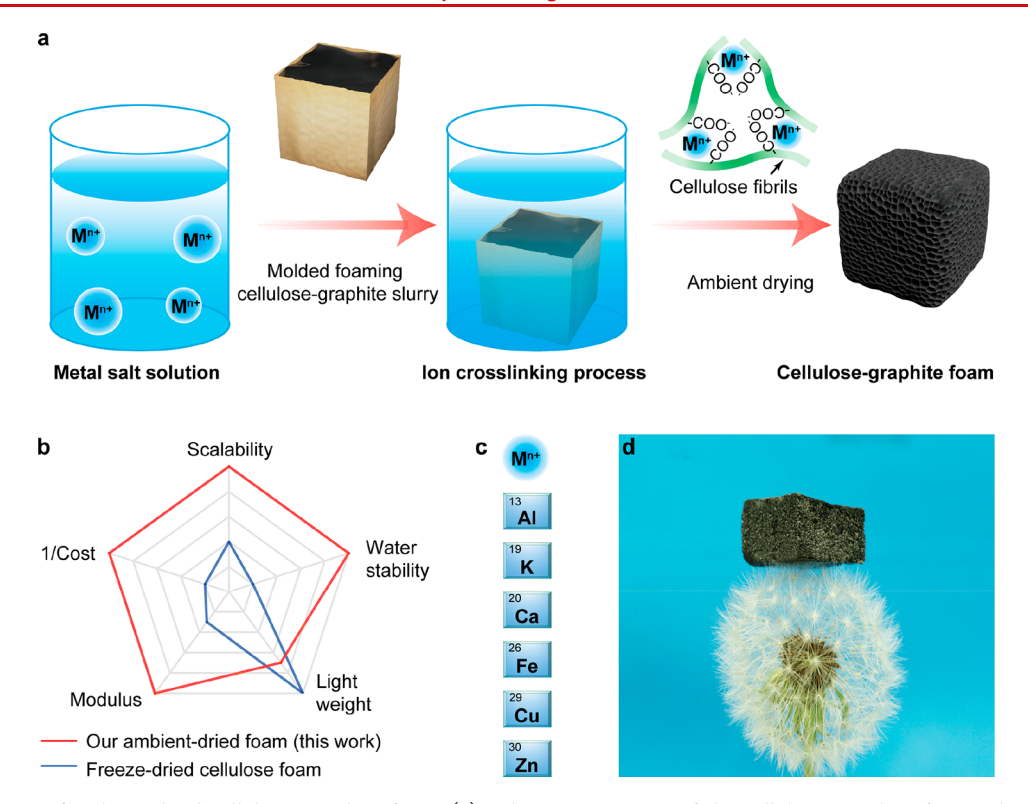


Figure 1. Schematic of ambient-dried cellulose—graphite foam. (a) Fabrication process of the cellulose—graphite foam. The paper box full of foaming slurry is immersed into metal salt solution to obtain 3D cross-linking networks, followed by ambient drying to fabricate porous foam. (b) Radar chart showing the advantages of our method for cellulose foam fabrication. (c) A range of metal ions can be used in this process. (d) Digital image of the cellulose—graphite foam staying on the top of a dandelion flower head, showcasing the ultralow density of the cellulose—graphite foam.

approach featuring cross-linking and ambient drying is highly efficient and scalable, which offers a sustainable route toward green foam production for a range of applications.

■ RESULTS AND DISCUSSION

In this cellulose-graphite foam design, graphite serves as the building block which is physically exfoliated and dispersed into the cellulose slurry. In a typical fabrication process, cellulosegraphite slurry with a solid content of 2 wt % is first prepared by ultrasonic mixing of the slurry containing graphite flakes and cellulose (Figure 1a). Sodium dodecyl sulfate (SDS) is added to the slurry to create sufficient air bubbles under stirring (Figure 1a and Figure S1). Upon the foam forming process, we transferred the bubbled cellulose-graphite suspension into a paper box and sank it into metal salt solution for molding, where the slurry gradually became stiff due to the cross-linking effect between negatively charged cellulose fibrils and the positively charged metal ions (Figure 1a). The stable three-dimensional (3D) cross-linking networks among the cellulose fibrils and metal ions could resist the increased capillary force and maintain the porous structure during ambient drainage. Finally a stable cellulose-graphite foam was achieved by fast ambient drying in air. The complete fabrication process, including foaming (1 min), molding/crosslinking (1 h), and ambient drying (8 h for foam size 4 cm \times 4 cm \times 2 cm), saves \sim 80% of the time used in freeze-drying for the sample with a similar size (e.g., > 48 h). Compared with the freeze-drying process, our approach enables ambient drying while it produces high-performance cellulose-graphite foam with advantageous scalability, cost, water stability, density, and compressive modulus (Figure 1b). Metal salt ions, including monovalent ion K⁺, divalent ions Ca²⁺/Zn²⁺/Cu²⁺, trivalent ions Al³⁺/Fe³⁺, are all effective in preparing the foam with high compressive strength (Figure 1c). The prepared cellulose—graphite foam features low density (~0.036 g·cm⁻³) that can stay on the top of a dandelion flower without any noticeable deformation (Figure 1d). Our fast, facile, and cost-effective approach to fabricate the cellulose—graphite foam demonstrates the following two key advantages: (1) good scalability and efficiency by using the ambient drying; (2) good water stability due to the cross-linking networks.

To understand the cross-linking interaction between the metal ions and the cellulose fibrils, 27,28 we added the cellulose-graphite droplets into deionized water and various metal salt solutions. Once immersed into deionized water, the edges of the droplets gradually turned blurry, as shown in Figure 2a and Figure S2. After shaking, all of the droplets in water disappeared and became cellulose-graphite suspension, which we attribute to the dissociation of the hydrogen bond between the cellulose fibrils (Figure 2b). However, the droplets of cellulose-graphite slurry are stabilized and maintained after dropping into the metal ions-containing solution, suggesting that the cellulose fibrils are cross-linked by metal ions to inhibit the dissociation of hydrogen bond between the cellulose fibrils. After shaking, the droplets in Na+and K⁺-containing solutions were collapsed, while the solutions with Ca2+, Zn2+, Cu2+, Al3+, or Fe3+ ions remained intact, indicating stronger cross-linking interaction. To quantitatively analyze the interaction between the cellulose fibrils and metal ions with different valences, we measured the mechanical properties of cellulose-graphite slurry with and without metal ions by the dynamic rheological tests (Figure 2c,d). For the

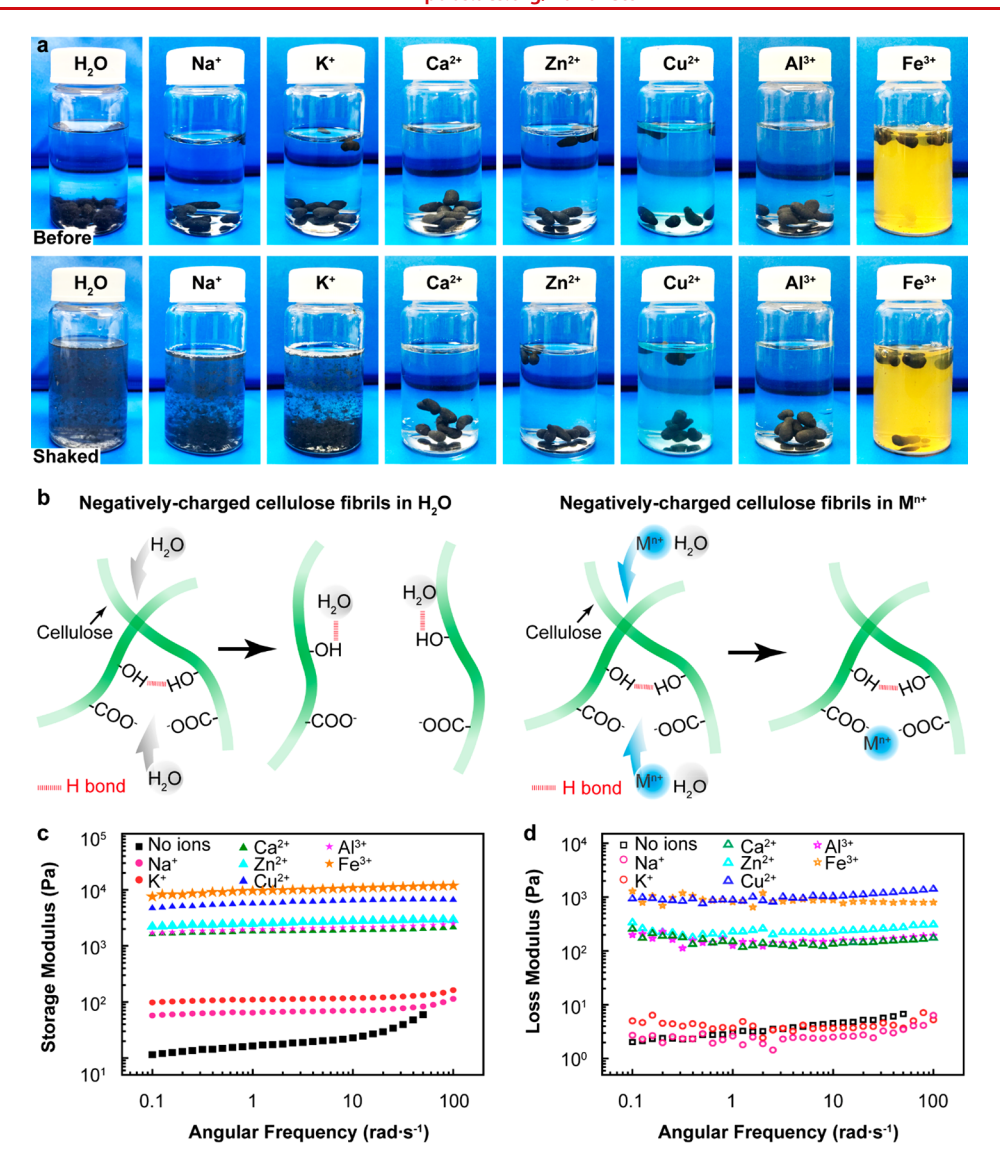


Figure 2. Characterization of the cellulose—graphite slurry with various metal ions. (a) Digital image of cellulose—graphite droplets in solutions containing various metal ions. (b) Schematic of the interaction between cellulose fibrils in solution with and without metal ions, showing the separated cellulose fibrils in bare water and the cross-linked cellulose fibrils in metal ion solutions. (c) Storage modulus as a function of angular frequency for the cellulose—graphite slurry treated by solutions with (0.05 M) and without metal ions. (d) Loss modulus as a function of angular frequency for the cellulose—graphite slurry treated by solutions with (0.05 M) and without metal ions.

cellulose—graphite slurry without ions, the storage and loss modulus gradually increase with the angular frequency, demonstrating a liquidlike behavior. However, the cellulose—graphite slurry with metal ions shows a constant storage and loss modulus that are independent of the frequency, implying a gel-like behavior because of the cross-linking interaction between cellulose fibrils and metal ions. Moreover, the storage modulus of cellulose—graphite slurry with the divalent and trivalent metal ions are 1–2 orders of magnitude higher than those with monovalent ions and without any ions, indicating that cross-linking interaction increases with higher valences. From the rheological tests, we conclude that the cross-linking interaction follows the order of Fe³⁺ > Cu²⁺ > Zn²⁺ > Al³⁺ > Ca²⁺ > K⁺ > Na⁺, consistent with our experimental results shown in Figure 2a.

On the basis of the cross-linking interaction between cellulose fibrils and metal ions, we fabricate the bulk cellulose—graphite foam through ambient drying process. First, the cubic paper molds containing foaming cellulose—

graphite slurry either directly dried (as a control, Figure 3a) or dried after cross-linking by metal ions (i.e., Fe³⁺) (Figure 3b) are compared. After removing the molds, only the foaming slurry soaked in Fe3+ solution turned into stiff and freestanding cellulose-graphite gel. Followed by ambient drying at 60 °C, the cellulose-graphite foam without ion treatment shows a collapsed film-like appearance (Figure 3a), whereas the foam with ion cross-linking exhibits a stable cubic shape (Figure 3b). Cross-sectional scanning electron microscopy (SEM) image of the cellulose-graphite foam without ion treatment displays large and collapsed pores, while that of the cellulose-graphite foam treated by Fe³⁺ shows uniform porous structure with pore size of ca. 200 μ m. In addition, the zoom-in SEM image clearly demonstrates the cellulose-graphite composite microstructure (Figure S3), where the exfoliated graphite flakes are embedded in the cellulose matrix. Note that the density of foam treated with Fe3+ (0.036 g·cm-3) is lower than the foam without ion treatment $(0.06 \text{ g} \cdot \text{cm}^{-3})$ due to the

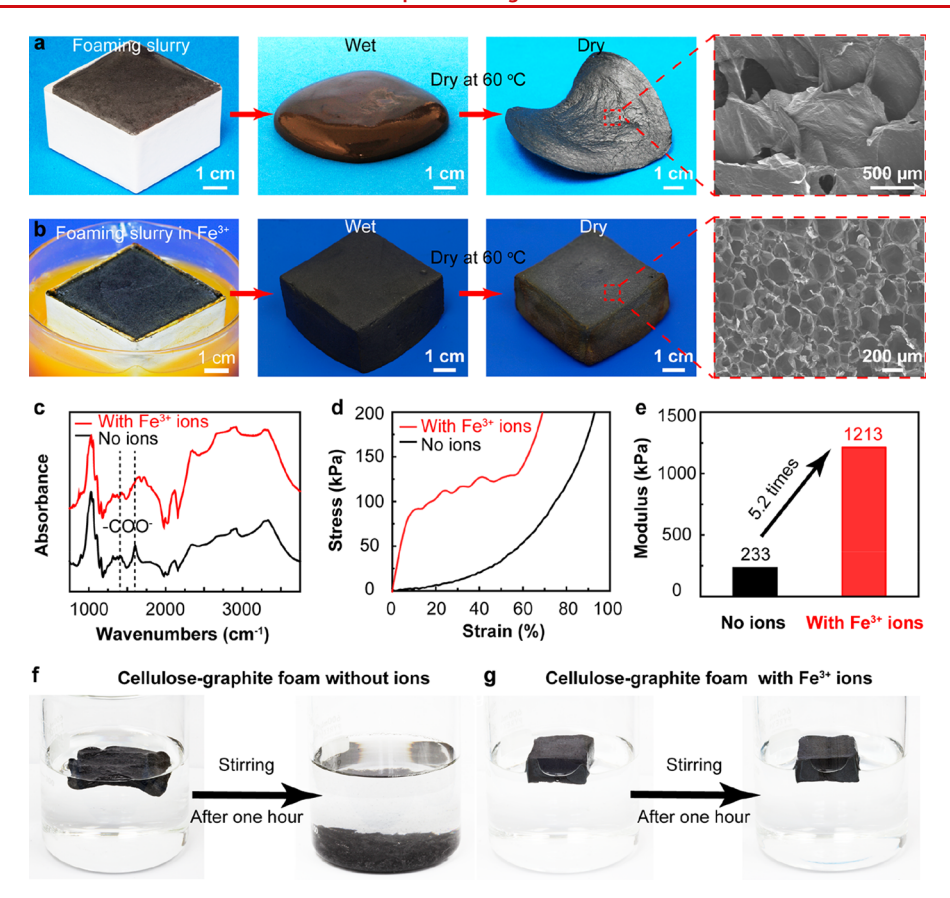


Figure 3. Fabrication and characterization of the cellulose—graphite foam. (a) Digital images of the fabrication process for the cellulose—graphite slurry without ion treatment and the SEM image of its microstructure. (b) Digital images of the fabrication process for the cellulose—graphite slurry with Fe^{3+} treatment and the SEM image of its microstructure. (c) FTIR spectra of foams with and without ion treatment. (d) Compressive stress—strain curves of foams with and without ion treatment. (e) The compressive modulus of foams with and without ion treatment. (f) Digital images of the foam without ion treatment before and after stirring for 1 h. (g) Digital images of the foam with ion treatment before and after stirring for 1 h.

highly porous structure. Using this method with different molds, various shapes of foam can be obtained (Figure S4).

We further characterized the composition, mechanical properties, and water stability of the cellulose-graphite foam with and without ion treatment. The Fourier-transform infrared spectroscopy (FTIR) spectra of the foam with and without Fe3+ treatment are collected to reveal the interaction between Fe3+ and cellulose fibrils (Figure 3c). The foam without ion treatment shows bands at 1407 and 1602 cm⁻¹ corresponding to the symmetric and asymmetric stretching vibrations of -COO-, respectively; in comparison, these bands for foam treated with Fe3+ showed a slight shift to higher wavenumbers and a decrease of intensity, suggesting interaction between the -COO⁻ group with Fe³⁺ by electrostatic attraction.²⁹ The elemental mapping by energy dispersive X-ray spectroscopy (EDS) shows that the Fe element is distributed uniformly (Figure S5). From the compressive stress-strain curves shown in Figure 3d, the foam treated with Fe3+ exhibits higher compressive stress and 5.2 times increase of modules compared to the foam without ion treatment (Figure 3e). The ion cross-linking network among cellulose fibrils by Fe3+ leads to stronger and stiffer cellular walls, resulting in higher mechanical strength of foam. Additionally, we evaluated the water stability of the cellulosegraphite foam by stirring the foam in water (Figure 3f,g). After 1 h of continuous stirring, the foam without ion treatment broke into small pieces, whereas the one treated with Fe3+ remained intact, demonstrating better water stability.

To demonstrate the universality of our method to fabricate cellulose-graphite foam, we immersed the foaming cellulosegraphite slurry mold in different solutions containing monovalent Na⁺/K⁺, divalent Ca²⁺/Zn²⁺/Cu²⁺, or trivalent Al3+. All of the prepared wet foams are free-standing and stiff, indicating successful cross-linking by the tested metal ions. After ambient drying, the foam with Na+ exhibits collapsed appearance with large pores, whereas the foam with K⁺ ions shows a well-shaped appearance and porous microstructure, potentially due to the stronger cross-linking interactions (Figure 4a). The dried foams treated with $Ca^{2+}/Zn^{2+}/Cu^{2+}/$ Al³⁺ ions all follow the cubic shape of the mold and exhibit sharp edges. The small pore size (200-400 μ m) observed in these cases further indicates that the divalent and trivalent ions played a key role in resisting the increased capillary forces and maintaining the porosity during the ambient drying process. We use EDS mapping on the dried foams treated with various ions to confirm their elemental distribution (Figures S6-8). Moreover, the densities of cellulose-graphite foams treated with different metal ions are compared in Figure 4b, among which foams treated with $K^+/Ca^{2+}/Zn^{2+}/Cu^{2+}/Al^{3+}$ ions show a similar density range (0.035-0.037 g·cm⁻³). We also characterized the compressive stress-strain curves of foams treated with different ions, where we found the foam treated with Fe3+ shows the highest compressive strength which is consistent with the trend of the storage modulus (Figure 2c). The high quality of cellulose foams cross-linked by a range of metal ions demonstrate the good universality of our approach.

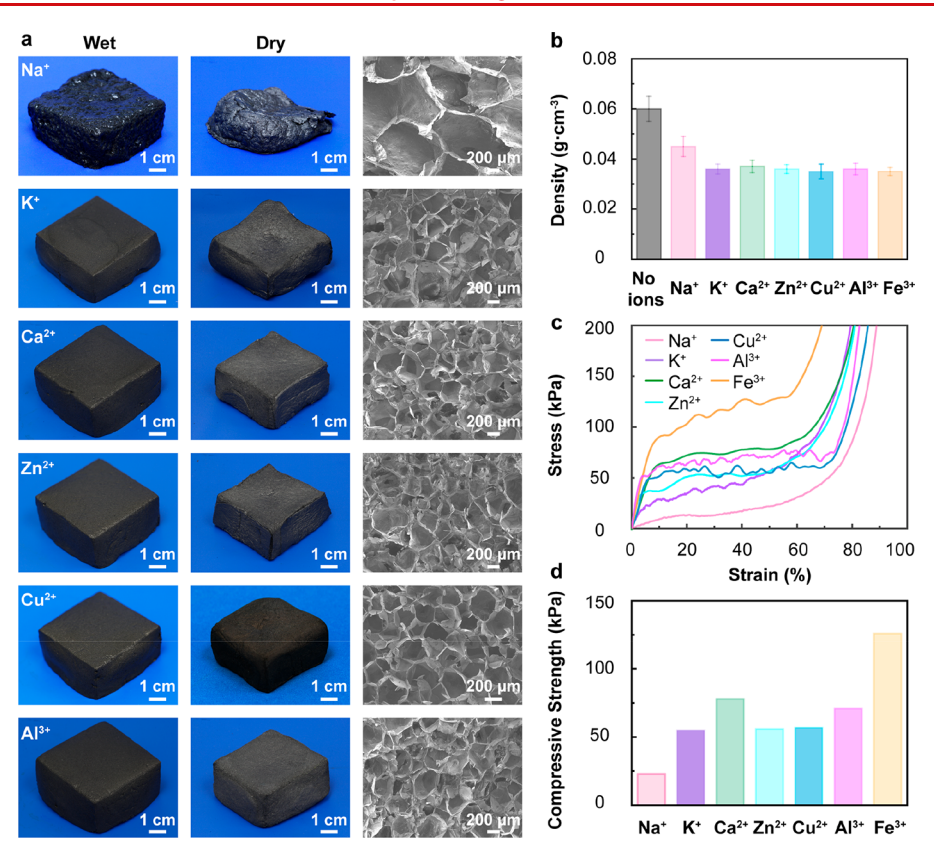


Figure 4. Characterization of cellulose–graphite foams stabilized by different ions. (a) Digital and SEM images of foams treated with monovalent K^+ , divalent $Ca^{2+}/Zn^{2+}/Cu^{2+}$, and trivalent Al^{3+} . (b) Density of the foams treated with different metal ions. (c) Compressive stress–strain curves of the foams treated with different metal ions. (d) Compressive strength of the foams treated with different metal ions at 50% strain.

To understand the effect of cross-linking by different metal ions, we conduct density functional theory (DFT) calculations implemented in the Vienna ab initio simulation package (VASP).30,31 The calculation was carried out with the exchange and correlation interaction parametrized by generalized gradient approximation (GGA) of the Perdew-Burke-Ernzerhof (PBE) functional (see Supporting Information for details).³² First, we focus on the effect of valence of the metal ions on the cross-linking interaction between the cellulose chains. Figures S9 and S10 show the simulation models of cellulose chains intercalated with different metal ions and the water molecule, respectively. Na+ and K+ tend to bond with one -COO group strongly and another -COO group weakly due to the lack of empty orbitals. In comparison, the divalent and trivalent metal ions bond with both O atoms in the two -COO groups, creating much stronger bonding. To quantitatively analyze the bonding, the binding energy and bond length between -COO⁻ and metal ions were calculated (Figure 5a,b). We found that the binding energy increases with the increase of valence in general, despite of Ca²⁺ showing an ultrahigh binding energy (-10.87 eV) among others. The trend is by and large consistent with the trend of compressive strengths (Figure 4c, d). The simulation also showed that the bond length decreases with the increase of valence. In particular, K+ has the largest bond length, which fits well with the density measurements (Figure 4b).

To better investigate the cross-linking interaction of different metal ions with the same valence, we calculate the charge density difference of the metal-ion-intercalated structure (Figures 5c-f, S11). we obtain the charge density difference (ρ_{Δ}) by using the equation $\rho_{\Delta} = \rho_{\text{total}} - \rho_{\text{ion}} - \rho_{\text{cellulose}}$, where

 $ho_{
m total},
ho_{
m ion}$, and $ho_{
m cellulose}$ are the total charge density of structure, the charge density of ions, and the charge density of cellulose, respectively. Both Na⁺ and K⁺ transfer electrons to the O atom in the -COO group. A few electrons are transferred from K to the -OH group, suggesting that bonding forms between -COO-, K+, and -OH (Figure 5c). Because of the lack of empty orbitals, it should be noted that the binding energy between two cellulose chains and alkali metal ions mainly comes from the restriction of the one chain possessing stronger bonding. At the same time, the binding energy between the other one and alkali metal ions is comparable to that between cellulose and water molecule (-0.83 eV). Thus, the sufficient water molecules in the solution can easily break the interaction between alkali metal ions and the weak cellulose chain, which results in the instability of the cross-linking network intercalated by Na⁺/ K⁺ ions. We noticed that the electron transfer in the Zn2+-intercalated cellulose can only occur between Zn²⁺ and the -COO⁻ groups (Figure 5d), while a similar but much higher electron transfer tendency happened between Ca²⁺ and the entire cellulose chains (Figure 5e). The extra electron transfer in the Ca²⁺-intercalated cellulose results in a much higher binding energy, thus the Ca2+ cross-linked cellulose foam has a higher strength than those cross-linked by other divalent ions (e.g., Zn²⁺). Our simulation found a higher electron transfer tendency between Al3+/ Fe3+ and the -COO groups than that by other ions (Na+, K+, Zn2+, Ca²⁺), resulting in the higher binding energy and strength, consistent with our experimental results. Because of the different donor sources of the orbital electron in Fe and Al, there exist divergences in the charge density of the ions. The -COO gains the electrons from the outermost electronic

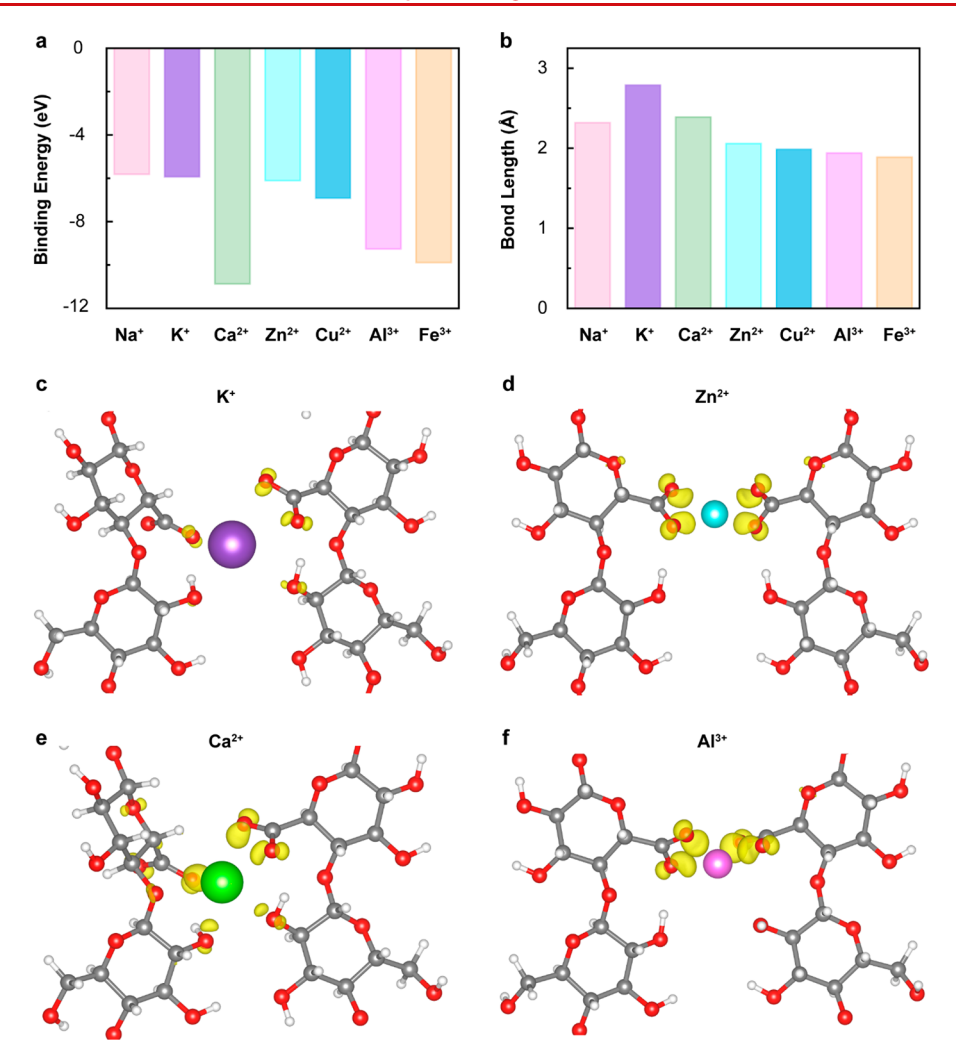


Figure 5. DFT simulation results. (a) Binding energy between cellulose and different metal ions. (b) Bond length between cellulose and different metal ions. Schematics showing charge density differences of metal ions-intercalated cellulose with (c) K^+ , (d) Zn^{2+} , (e) Ca^{2+} , and (f) Al^{3+} . The yellow region represents the gain of electrons.

orbit of the Al^{3+} . At the same time, the Fe^{3+} , as the transition element, donates the electrons from both 4s and 3d electronic orbits, which in turn increases the outermost charge densities of Fe^{3+} .

■ CONCLUSION

In this work, a facile and scalable approach featuring ion crosslinking followed by ambient drying is developed to fabricate light-density, robust, and biodegradable cellulose-graphite foams. Because of the 3D ion cross-linking networks established by the electrostatic interaction between metal ions and negatively charged cellulose fibrils, the wet cellulosegraphite foam could resist the increased capillary forces during the ambient drying process. Remarkably, the cellulosegraphite foam cross-linked by Fe3+ shows a porous microstructure (mean pore size $\sim 200 \mu m$), high dissociation resistibility in water, and high compressive modules (1213 kPa) compared with the foam without ion cross-linking treatment. In addition, monovalent K+ ions, divalent Ca2+, Zn²⁺, Cu²⁺ ions, and trivalent Al³⁺ ions can all be used to prepare cellulose-graphite foam with uniform porous structure and high compressive strengths, demonstrating good universality of our approach. DFT calculations show that the binding energy of different metal ions intercalated with the cellulose

chains follows the order of $Ca^{2+} > Fe^{3+} > Al^{3+} > Cu^{2+} > Zn^{2+} > K^+ > Na^+$, consistent with our experimental observation. Our approach demonstrates great potential for the cost-effective, energy-efficient, and scalable production of sustainable foam materials for a range of applications.

ASSOCIATED CONTENT

Supporting Information

The Supporting Information is available free of charge at https://pubs.acs.org/doi/10.1021/acs.nanolett.2c00167.

Experimental section; supplementary figures including digital images, SEM images, EDS results, simulation model, and charge density difference (PDF)

AUTHOR INFORMATION

Corresponding Authors

Liangbing Hu — Department of Materials Science and Engineering, University of Maryland, College Park, Maryland 20742, United States; Center for Materials Innovation, University of Maryland, College Park, Maryland 20742, United States; ocid.org/0000-0002-9456-9315; Email: binghu@umd.edu

Nano Letters pubs.acs.org/NanoLett Letter

Teng Li — Department of Mechanical Engineering, University of Maryland, College Park, Maryland 20742, United States; orcid.org/0000-0001-6252-561X; Email: lit@umd.edu

Authors

- Ruiliu Wang Department of Materials Science and Engineering, University of Maryland, College Park, Maryland 20742, United States
- Chaoji Chen Department of Materials Science and Engineering, University of Maryland, College Park, Maryland 20742, United States; orcid.org/0000-0001-9553-554X
- Zhenqian Pang Department of Mechanical Engineering, University of Maryland, College Park, Maryland 20742, United States
- Xizheng Wang Department of Materials Science and Engineering, University of Maryland, College Park, Maryland 20742, United States
- Yubing Zhou Department of Materials Science and Engineering, University of Maryland, College Park, Maryland 20742, United States
- Qi Dong Department of Materials Science and Engineering, University of Maryland, College Park, Maryland 20742, United States
- Miao Guo Department of Materials Science and Engineering, University of Maryland, College Park, Maryland 20742, United States
- Jinlong Gao Department of Materials Science and Engineering, University of Maryland, College Park, Maryland 20742, United States
- Upamanyu Ray Department of Mechanical Engineering, University of Maryland, College Park, Maryland 20742, United States
- Qinqin Xia Department of Materials Science and Engineering, University of Maryland, College Park, Maryland 20742, United States
- Zhiwei Lin Department of Materials Science and Engineering, University of Maryland, College Park, Maryland 20742, United States
- Shuaiming He Department of Materials Science and Engineering, University of Maryland, College Park, Maryland 20742, United States
- Bob Foster Trinity Industries, Inc., Dallas, Texas 75207, United States

Complete contact information is available at: https://pubs.acs.org/10.1021/acs.nanolett.2c00167

Author Contributions

^aR.W., C.C., Z.P., and X.W. contributed equally to this work. **Author Contributions**

L.H., R.W., C.C., and Y.Z. designed the experiments. R.W. and U.R. prepared the cellulose—graphite slurry. R.W. and Y.Z. carried out foam fabrication experiments and measured mechanical properties. T.L. and Z.P. conducted the DFT calculation. J.G. provided the digital images of samples. Q.X. and S.H. conducted the FTIR test. J.G. and Z.L. created the 3D illustrations. L.H., R.W., Q.D., T.L., C.C., and X.W. collectively wrote the paper with comments from all authors. All authors commented on the final manuscript.

Notes

The authors declare no competing financial interest.

ACKNOWLEDGMENTS

The authors acknowledge the support of U.S. National Science Foundation (Grant Nos. 1362256 and 1936452) and Trinity Industries Inc. The authors acknowledge the support of the Maryland Nanocenter and Advanced Imaging and Microscopy (AIM) Lab. T.L. and Z.P. acknowledge the University of Maryland supercomputing resources (http://hpcc.umd.edu) and Maryland Advanced Research Computing Center (MARCC) made available for conducting the research reported in this paper.

REFERENCES

- (1) Wicklein, B.; Kocjan, A.; Salazar-Alvarez, G.; Carosio, F.; Camino, G.; Antonietti, M.; Bergstrom, L. Thermally Insulating and Fire-Retardant Lightweight Anisotropic Foams Based on Nanocellulose and Graphene Oxide. *Nat. Nanotechnol.* **2015**, *10* (3), 277–83.
- (2) Si, Y.; Wang, X.; Dou, L.; Yu, J.; Ding, B. Ultralight and Fire-Resistant Ceramic Nanofibrous Aerogels with Temperature-Invariant Superelasticity. *Sci. Adv.* **2018**, *4* (4), No. eaas8925.
- (3) Cao, L.; Si, Y.; Yin, X.; Yu, J.; Ding, B. Ultralight and Resilient Electrospun Fiber Sponge with a Lamellar Corrugated Microstructure for Effective Low-Frequency Sound Absorption. ACS Appl. Mater. Interfaces 2019, 11 (38), 35333–35342.
- (4) Mao, J.; Iocozzia, J.; Huang, J.; Meng, K.; Lai, Y.; Lin, Z. Graphene Aerogels for Efficient Energy Storage and Conversion. *Energy Environ. Sci.* **2018**, *11* (4), 772–799.
- (5) Hu, X.; Xu, W.; Zhou, L.; Tan, Y.; Wang, Y.; Zhu, S.; Zhu, J. Tailoring Graphene Oxide-Based Aerogels for Efficient Solar Steam Generation under One Sun. *Adv. Mater.* **2017**, 29 (5), 1604031.
- (6) Barrios, E.; Fox, D.; Li Sip, Y. Y.; Catarata, R.; Calderon, J. E.; Azim, N.; Afrin, S.; Zhang, Z.; Zhai, L. Nanomaterials in Advanced, High-Performance Aerogel Composites: A Review. *Polymers* **2019**, *11* (4), 726.
- (7) Ferreira, F. V.; Otoni, C. G.; De France, K. J.; Barud, H. S.; Lona, L. M. F.; Cranston, E. D.; Rojas, O. J. Porous Nanocellulose Gels and Foams: Breakthrough Status in the Development of Scaffolds for Tissue Engineering. *Mater. Today* **2020**, *37*, 126–141.
- (8) Suh, K. W.; Park, C. P.; Maurer, M. J.; Tusim, M. H.; Genova, R. D.; Broos, R.; Sophiea, D. P. Lightweight Cellular Plastics. *Adv. Mater.* **2000**, *12* (23), 1779–1789.
- (9) Wang, C.; Xiong, Y.; Fan, B.; Yao, Q.; Wang, H.; Jin, C.; Sun, Q. Cellulose as an Adhesion Agent for the Synthesis of Lignin Aerogel with Strong Mechanical Performance, Sound-Absorption and Thermal Insulation. *Sci. Rep.* **2016**, *6*, 32383.
- (10) Kuang, T.; Chang, L.; Chen, F.; Sheng, Y.; Fu, D.; Peng, X. Facile Preparation of Lightweight High-Strength Biodegradable Polymer/Multi-Walled Carbon Nanotubes Nanocomposite Foams for Electromagnetic Interference Shielding. *Carbon* **2016**, *105*, 305–
- (11) Li, T.; Chen, C.; Brozena, A. H.; Zhu, J. Y.; Xu, L.; Driemeier, C.; Dai, J.; Rojas, O. J.; Isogai, A.; Wagberg, L.; Hu, L. Developing Fibrillated Cellulose as a Sustainable Technological Material. *Nature* **2021**, *590* (7844), 47–56.
- (12) Mukhopadhyay, A.; Cheng, Z.; Natan, A.; Ma, Y.; Yang, Y.; Cao, D.; Wang, W.; Zhu, H. Stable and Highly Ion-Selective Membrane Made from Cellulose Nanocrystals for Aqueous Redox Flow Batteries. *Nano Lett.* **2019**, *19* (12), 8979–8989.
- (13) Guan, Q.-F.; Yang, H.-B.; Han, Z.-M.; Zhou, L.-C.; Zhu, Y.-B.; Ling, Z.-C.; Jiang, H.-B.; Wang, P.-F.; Ma, T.; Wu, H.-A.; Yu, S.-H. Lightweight, Tough, and Sustainable Cellulose Nanofiber-Derived Bulk Structural Materials with Low Thermal Expansion Coefficient. *Sci. Adv.* **2020**, *6* (18), No. eaaz1114.
- (14) Guan, Q.-F.; Yang, H.-B.; Han, Z.-M.; Ling, Z.-C.; Yu, S.-H. An All-Natural Bioinspired Structural Material for Plastic Replacement. *Nat. Commun.* **2020**, *11* (1), 5401.

Nano Letters pubs.acs.org/NanoLett Letter

- (15) Hou, Y.; Guan, Q. F.; Xia, J.; Ling, Z. C.; He, Z.; Han, Z. M.; Yang, H. B.; Gu, P.; Zhu, Y.; Yu, S. H.; Wu, H. Strengthening and Toughening Hierarchical Nanocellulose Via Humidity-Mediated Interface. ACS Nano 2021, 15 (1), 1310-1320.
- (16) Klemm, D.; Heublein, B.; Fink, H.-P.; Bohn, A. Cellulose: Fascinating Biopolymer and Sustainable Raw Material. Angew. Chem., Int. Ed. 2005, 44 (22), 3358-3393.
- (17) Kontturi, E.; Laaksonen, P.; Linder, M. B.; Nonappa; Gröschel, A. H.; Rojas, O. J.; Ikkala, O. Advanced Materials through Assembly of Nanocelluloses. Adv. Mater. 2018, 30 (24), 1703779.
- (18) Li, Y.; Zhu, H.; Shen, F.; Wan, J.; Lacey, S.; Fang, Z.; Dai, H.; Hu, L. Nanocellulose as Green Dispersant for Two-Dimensional Energy Materials. Nano Energy 2015, 13, 346-354.
- (19) Budtova, T. Cellulose Ii Aerogels: A Review. Cellulose 2019, 26 (1), 81-121.
- (20) Ferreira, E. S.; Cranston, E. D.; Rezende, C. A. Naturally Hydrophobic Foams from Lignocellulosic Fibers Prepared by Oven-Drying. ACS Sustain. Chem. Eng. 2020, 8 (22), 8267-8278.
- (21) Zhao, S.; Malfait, W. J.; Guerrero-Alburquerque, N.; Koebel, M. M.; Nyström, G. Biopolymer Aerogels and Foams: Chemistry, Properties, and Applications. Angew. Chem., Int. Ed. 2018, 57 (26), 7580-7608.
- (22) Yang, L.; Mukhopadhyay, A.; Jiao, Y.; Yong, Q.; Chen, L.; Xing, Y.; Hamel, J.; Zhu, H. Ultralight, Highly Thermally Insulating and Fire Resistant Aerogel by Encapsulating Cellulose Nanofibers with Two-Dimensional Mos₂. Nanoscale 2017, 9 (32), 11452-11462.
- (23) Pääkkö, M.; Vapaavuori, J.; Silvennoinen, R.; Kosonen, H.; Ankerfors, M.; Lindström, T.; Berglund, L. A.; Ikkala, O. Long and Entangled Native Cellulose I Nanofibers Allow Flexible Aerogels and Hierarchically Porous Templates for Functionalities. Soft Matter 2008, 4 (12), 2492-2499.
- (24) Cervin, N. T.; Aulin, C.; Larsson, P. T.; Wagberg, L. Ultra Porous Nanocellulose Aerogels as Separation Medium for Mixtures of Oil/Water Liquids. Cellulose 2012, 19 (2), 401-410.
- (25) Li, S.-C.; Hu, B.-C.; Ding, Y.-W.; Liang, H.-W.; Li, C.; Yu, Z.-Y.; Wu, Z.-Y.; Chen, W.-S.; Yu, S.-H. Wood-Derived Ultrathin Carbon Nanofiber Aerogels. Angew. Chem., Int. Ed. 2018, 57 (24), 7085-7090
- (26) Zu, G.; Shen, J.; Zou, L.; Wang, F.; Wang, X.; Zhang, Y.; Yao, X. Nanocellulose-Derived Highly Porous Carbon Aerogels for Supercapacitors. Carbon 2016, 99, 203-211.
- (27) Dong, H.; Snyder, J. F.; Williams, K. S.; Andzelm, J. W. Cation-Induced Hydrogels of Cellulose Nanofibrils with Tunable Moduli. Biomacromolecules 2013, 14 (9), 3338-3345.
- (28) Guo, Y.; Bae, J.; Fang, Z.; Li, P.; Zhao, F.; Yu, G. Hydrogels and Hydrogel-Derived Materials for Energy and Water Sustainability. Chem. Rev. 2020, 120 (15), 7642-7707.
- (29) Zhu, C.; Soldatov, A.; Mathew, A. P. Advanced Microscopy and Spectroscopy Reveal the Adsorption and Clustering of Cu(Ii) onto Tempo-Oxidized Cellulose Nanofibers. Nanoscale 2017, 9 (22), 7419-7428.
- (30) Kresse, G.; Furthmüller, J. Efficient Iterative Schemes for Ab Initio Total-Energy Calculations Using a Plane-Wave Basis Set. Phys. Rev. B 1996, 54 (16), 11169.
- (31) Kresse, G.; Hafner, J. Ab Initio Molecular Dynamics for Liquid Metals. Phys. Rev. B 1993, 47 (1), 558.
- (32) Perdew, J. P.; Burke, K.; Ernzerhof, M. Generalized Gradient Approximation Made Simple. Phys. Rev. Lett. 1996, 77 (18), 3865-3868.

□ Recommended by ACS

Top-Down Approach Making Anisotropic Cellulose Aerogels as Universal Substrates for Multifunctionalization

Jonas Garemark, Yuanyuan Li, et al.

MAY 15, 2020 ACS NANO

RFAD 🗹

Cellulose-Based Hybrid Structural Material for **Radiative Cooling**

Yipeng Chen, Huiqiao Li, et al.

DECEMBER 10, 2020

NANO LETTERS

READ **C**

Exploring the Hierarchical Structure and Alignment of Wood Cellulose Fibers for Bioinspired Anisotropic Polymeric Composites

Râmile Luíse Pereira Oliveira Moreira, Mathias Strauss, et al.

FERRUARY 28 2020

ACS APPLIED BIO MATERIALS

READ C

Mechanisms of Cellulose Fiber Comminution to Nanocellulose by Hyper Inertia Flows

Jakob D. Redlinger-Pohn, L. Daniel Söderberg, et al.

JANUARY 04, 2022

ACS SUSTAINABLE CHEMISTRY & ENGINEERING

RFAD 🗹

Get More Suggestions >